04,09

Analysis of dielectric spectra taking into account the distribution of relaxers over relaxation times

© A.V. Ilyinsky, E.B. Shadrin

Ioffe Institute,
St. Petersburg, Russia

E-mail: shadr.solid@mail.ioffe.ru

Received March 12, 2024
Revised April 10, 2024
Accepted April 11, 2024

A numerical analysis of the features of the dielectric spectra of crystalline substances deposited on insulating substrates, excluding the possibility of through-current flow, is carried out. The analysis is based on the use of the distribution function of the numbers of relaxers according to their relaxation times. It is shown that the principles of numerical analysis are different for different types of features of dielectric spectra. The Gavrilyak–Negami function is used to analyze features occupying narrow frequency ranges ($\Delta\omega \leq 1$ order of magnitude ω).For wider ranges ($\Delta\omega \sim 2-3$ orders of magnitude), the improved Gavrilyak–Negami function is used.For the broadest features ($\Delta\omega > 3$ orders of magnitude), the role of the distribution function is played by the function of the frequency dependence of the imaginary part of the dielectric constant $\varepsilon''(f)$, which is obtained experimentally.Before use, this function is converted to the function $\varepsilon''(\tau)$, and the shape of this function is adjusted using a special algorithm.

Keywords: dielectric spectroscopy, complex permittivity, dielectric loss angle tangent, Debye distribution, Gavrilyak–Negami function.

DOI: 10.61011/PSS.2024.05.58498.51

1. Introduction

Dielectric spectra (DS) analysis is limited to processing of the electrical response of crystalline and amorphous materials to low-frequency sinusoidal electric field. For the experimental dielectric spectroscopy method, frequency profile functions of the complex permittivity components of the test material are the main and most informative spectra elements that carry maximum information. $\varepsilon^*(\omega) = \varepsilon'(\omega) + i\varepsilon''(\omega)$ (here, $\omega = 2\pi f$, where f is the probing electric field oscillation frequency, i is the imaginary unit) [1–3].

More specifically, — of interest are: the dielectric loss angle tangent $\mathrm{tg}\,\delta(f) = \varepsilon''(f)/\varepsilon'(f)$ and differential function of relaxation time distribution density by numerical values that, as will be shown, may be constructed using the data on $\varepsilon''(f)$. The dielectric loss angle tangent $\mathrm{tg}\,\delta(f) = \varepsilon''/\varepsilon'$ is defined as the ratio between the imaginary part of the material's complex permittivity $\varepsilon''(f)$ and its real part $\varepsilon'(f)$. When a material sample that has little if any energy loss is placed in the measuring cell of a dielectric spectrometer, the phase angle between bias current and sinusoidal voltage applied to the cell is equal to $\psi = \pi/2$. The bias current oscillations lead in phase by this angle the sinusoidal voltage applied to the cell. At the same time, a non-ideal dielectric reduces the phase angle by δ due to the presence of dielectric loss in the sample, so $\psi = \pi/2 - \delta$. Reduction of loss is followed by the decrease of δ that widely varies for different materials. Achievement of a possibly lower angle δ is essential when using such materials in many devices and, in particular, in high-quality instrumentation.

The previous decades have shown that detailed scientific study of properties of various materials appeared to be impossible without using the dielectric spectroscopy methods. This resulted in design and successful creation of a constellation of next generation high-quality industrial dielectric spectrometers. Modern nanomaterials and high-speed computers using advanced software played a vital role in this process.

It should be noted that many studies containing the experimental DS are limited to the Debye distribution when analyzing relaxation processes discussed herein and possible causes of DS features broadening are discussed on the qualitative level only. There are also computational studies [4–10] devoted to the DS analysis on the basis of the Cole–Cole diagrams (CC diagrams), Davison functions, Gavrilyak–Negami (GN function) functions, etc., but most of them is based on mathematical algorithms constructed using empirical data. At the same time, many studies of dielectric spectroscopy devoted to the analysis of the distribution function of the number of relaxers by their times based on the analysis of the GN function do not contain any step-by-step calculation of the shape and features of experimental DS. It is apparent that computational methods shall be used correctly for such calculations and this is a separate problem.

The foregoing has defined the purpose of this study that is limited to the demonstration of relaxation process simulation principle based on the opportunities offered by the computational methods used in the DS spectra. Discussion in the proposed paper is subject to the following algorithm.

1. At the initial stage, the constructed model assumes that there is DS — frequency dependence of complex

permittivity components $\varepsilon^*(\omega)$ and it is assumed that there is no any relaxation-time distribution of relaxer density. This version corresponds to the Debye model according to which there is a single typical time of system relaxation response τ_D to an external probing impact that is the same for all relaxers. At the next stage, a problem is set out to expand the computational capabilities of the model through the analysis of the case with several types of relaxers with each of them obeying the Debye distribution law. For example, with two types of relaxers whose relaxation times τ_{D1} and τ_{D2} are widely spaced on the time scale. This problem is solved in the DS analysis by simple summation of two expressions describing the Debye distribution.

2. The next simulation stage is limited to introduction, instead of theδ-function used in the Debye distribution, of a broadened distribution of the Debye type relaxers simulated according to empirical analytical expressions. Such broadened distribution is intended to analyze the features of real DS more adequately.

3. At the next simulation stage, continuous relaxation-time distribution of relaxers is introduced. In this case, the sum is replaced with an integral and the weight function $G(\tau)$ is introduced under the integral to define the contribution of each type of relaxers to the common result. Frequency dependence function of permittivity is calculated at tis stage by the expression

$$\varepsilon^*(\omega) = \varepsilon_\infty + \Delta\varepsilon \int_0^\infty \frac{G(t)}{1 + i\omega\tau}\, d\tau. \qquad (1)$$

4. Further improvement of the proposed model is limited to simulation of the weight function that is most suitable for calculations. In particular, for this purpose the Gavrilyak–Negami (GN) distribution function [11–14] may be used that has adjustable parameters τ_{HN}, α_{HN} and β_{HN} whose variation is intended to ensure coincidence between the calculation and experiment. However, the detailed analysis performed at the next stage of construction of the proposed design model demonstrates an important consideration that the choice of adjustable parameters that ensure the same integration result according to (1) is ambiguous.

5. It is also important that other types of weight functions that differ in form from the GN function give the same result during integration as that when using the GN function. This situation suggests that solution of inverse search problem $G(\tau)$ — relaxer time-distribution function — is not unambiguous.

6. The next stage is devoted to validity check of this assertion and is limited to integration according to expression (1) which is satisfied for a set of various functions used as the weight function $G(\tau)$. And when almost any mathematically „good“ analytical function $G(\tau)$ is chosen, integration gives a result that almost coincides with the same function $G(\tau)$ that has been introduced under the integral as a weight function! Such repeatability suggests that expression (1) actually represents a filtration equation version of $G(\tau)$ used in the classical function filtration method through the Dirac δ-function [15–18], though, except that in (1) the Debye function is used as a filtration function. Being a classical distribution in the relaxation theory, the Debye distribution is not a high-quality filter due to the finite width of the Debye distribution and asymmetry inherent in it. This fact results in correction of the weight function $G(\tau)$ to achieve the acceptable coincidence between the integration result and experiment after fitting. Therefore, software of modern dielectric spectrometers is able to use the experimental function $\varepsilon''(f)$ as $G(\tau)$, where f is replaced with τ, and get an acceptable result after integration and correction of the form of $\varepsilon''(\tau)$.

2. Debye dielectric spectra

At the initial stage, the constructed design model assumes that the features of DS are qualitatively, and sometimes quantitatively, described by the Debye equation [1–3]:

$$\varepsilon^*(\omega) = \varepsilon_\infty + \frac{\Delta\varepsilon}{[1 + i\omega\tau_D]}, \qquad (2)$$

where ω is the cyclic frequency, τ_D relaxation time, $\Delta\varepsilon = \varepsilon'_\infty - \varepsilon'_0$, i is the imaginary unit.

One (or more) peak(s) on the frequency dependence of the imaginary part of permittivity $\varepsilon''(f)$, one (several) step(s) for the real part $\varepsilon'(f)$ and one (or more) semicircle(s) $\varepsilon''(\varepsilon')$ on the CC diagram correspond to the presence of one (or more) types of relaxers. When interpreting the DS measurements, certain physical nature of each type of relaxers are identified through the analysis of all available experimental and theoretical data on the test material, including the data acquired by other investigation methods. It should be noted that one individual peak on the frequency dependence of the imaginary part of permittivity $\varepsilon''(f)$ is assigned to each type of relaxers. For this, it is assumed that such peak may be isolated unambiguously in the experimental DS according to the Rayleigh criterium.

Figure 1 illustrates $\varepsilon' = \varepsilon_\infty + \Delta\varepsilon/[1 + (\omega\tau_D)^2]$, $\varepsilon'' = \Delta\varepsilon \cdot \omega\tau_D/[1 + (\omega\tau_D)^2]$ and $\varepsilon''(\varepsilon')$ spectra plotted for $f = \omega/(2\pi)$ in the logarithmic scale in accordance with equation (2) for one type of relaxers with a single relaxation time τ_D. Features of DS in this case represent a relatively narrow (not more than one order of variation of f) peak of $\varepsilon''(f)$, a clearly pronounced step with the same width on $\varepsilon'(f)$ curve and a regular semicircle of the CC diagram: $\varepsilon''(\varepsilon')$.

Variables of equation (2) are chosen for the analysis in such a way as to ensure correspondence of the design curves in shape to the experimental curves and, in particular, congruence of the Debye frequency $f = 1/(2\pi\tau_D)$ with the frequency position of fmax peak on the experimental function $\varepsilon''(f)$. It should be noted that the next simulation stages use typical relaxation times of about $1.6 \cdot 10^{-4}$ s (τ_{HN}, τ_D) that correspond to 10^3 Hz lying in the center of the frequency range (10^{-2}–10^7 Hz) of the dielectric spectrometer.

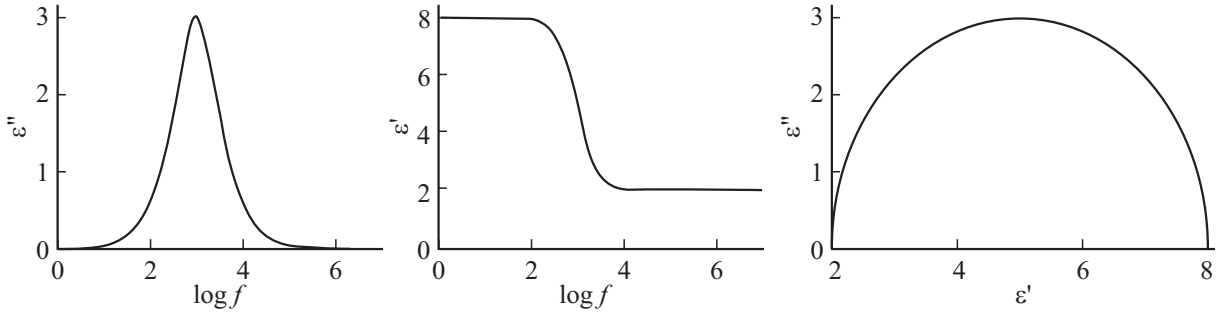

Figure 1. Frequency dependences ε'', ε' and the Cole–Cole diagram — $\varepsilon''(\varepsilon')$ plotted using equation (2). $\tau_D = 1.6 \cdot 10^{-4}$ s.

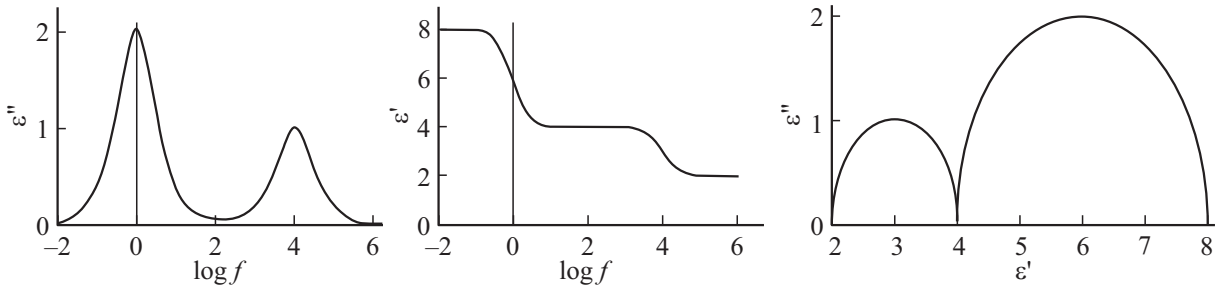

Figure 2. Frequency dependences $\varepsilon''(f)$, $\varepsilon'(f)$ and the Cole–Cole diagram — $\varepsilon''(\varepsilon')$ plotted using equation (3). $\tau_{D1} = 1.6 \cdot 10^{-1}$ s, $\tau_{D2} = 1.6 \cdot 10^{-5}$ s.

At the next stage, for adequate description of the DS measurements with two peaks that correspond to the presence of two types of relaxers in the test material, expression (2) is transformed into expression (3) that takes into account the superposition of two relaxation processes with relaxation times, respectively, τ_{D1} and τ_{D2}:

$$\varepsilon^*(\omega) = \varepsilon_\infty + \frac{\Delta\varepsilon_1}{[1 + (i\omega\tau_{D1})]} \frac{\Delta\varepsilon_2}{[1 + (i\omega\tau_{D2})]}. \qquad (3)$$

$\varepsilon'(f)$, $\varepsilon''(f)$ and $\varepsilon''(\varepsilon')$ curves, i.e. dielectric spectra (DS) plotted according to (3) are shown in Figure 2. These DS also contain two narrow non-overlapping peaks on $\varepsilon''(f)$ curve, two clearly distinguished steps on $\varepsilon'(f)$ curve and two regular semicircles on the Cole-Cole — diagram $\varepsilon''(\varepsilon')$.

3. DS analysis using empirical analytical expressions

Comparison of the DS measurements within the Debye theory performed at the initial simulation stage with the experiment results shows that the peaks and steps on the experimental frequency dependences $\varepsilon''(t)$ and $\varepsilon'(f)$ appear to at least half as wide (in the logarithmic scale) as on the design curves and the measured CC diagrams do not look like regular semicircles; i.e. „heights“ of the experimental CC semicircles are lower than their half „widths“ by 10–30%. Considering the foregoing, to make the calculations more consistent with the measurements, expressions (2) or (3) are modified at the next stage by using equation (4) [11,15]:

$$\varepsilon^*(\omega) = \varepsilon_\infty + \frac{\Delta\varepsilon}{[1 + (i\omega\tau)^2]^\beta}. \qquad (4)$$

Here, α and β are variables that lie in the range from 0 to 1 and are used to adjust, by varying them, the design halfwidth and shape of the features of $\varepsilon'(f)$ and $\varepsilon''(f)$ to the measurements. The experience shows that, though the selection of α and β values and their specific physical significance are ambiguous, complication of equation (2) by this method that transforms it to equation (4) appears to be helpful for classification of a wider set of experimental DS. And, moreover, when fitting α and β, equation (4) may be used to represent the experimental data in the analytical form together with representation in the form of tables and curves.

4. DS analysis using the function of relaxation-time distribution of the numbers of relaxers

The next stage of design modeling uses the analysis of the general fitting method for the calculation and experimental data. For this, function $G(\tau)$ is introduced that has physical significance of the relaxation-time distribution of relaxers or each individual type of relaxers. In this case, the expression for the frequency dependence of complex permittivity (equation (2)) is written as (1). note that

expressions (1) and (2) appear to be identical in case when $G(\tau)$ represents the Dirac δ-function (filtering property of δ-function [16]).

A specific form of $G(\tau)$ may vary widely, however, all possible variations shall satisfy a set of general requirements. In particular, $G(\tau)$ shall have a single peak for each type of relaxer. Moreover, is shall decline smoothly on both sides of its peak such that $\lim[G(\tau)] = 0$ at $\tau \to 0$ and $\tau \to \infty$. Such function, in principle, may be constructed even as a curve, digitized, normalized and introduced as a digital array into equation (1) using the corresponding software package. The experience of such approach shows that good agreement of the design and experimental data may be achieved by varying a particular form of the proposed curve (width, asymmetry, position on the frequency scale).

Therefore, the wide variation capability of $G(\tau)$ adequately describing the experiment indicates that there is no reliable algorithm for acquisition of data on the structure of $G(\tau)$ through the analysis of the experimental DS. And this, in turn, means that the optimum form of $G(\tau)$ shall be constructed using additional considerations, for example, detailed analysis of physical mechanisms defining the specific relaxation processes in the test material.

Though such approach seems to be quite sophisticated, it appears to be, as proven in real practice, fairly executable. However, when using the computational algorithms described herein, a question naturally arises regarding what shall be used as the initial form of $G(\tau)$? A wide variety of options may be offered in response to this question. Some of them are discussed in detail below.

5. Gavrilyak–Negami function $g_{\mathrm{HN}}(\tau)$

One of the options is in using the GN function — $g_{\mathrm{HN}}(\tau)$ as the weight function $G(\tau)$ [11], with the analytical expression written as:

$$g_{\mathrm{HN}}(\tau) = \frac{\left(\frac{\tau}{\tau_{\mathrm{HN}}}\right)^{\beta_{\mathrm{HN}}\alpha_{\mathrm{HN}}} \sin(\beta_{\mathrm{HN}}\Theta)}{\pi\tau\left(\left(\frac{\tau}{\tau_{\mathrm{HN}}}\right)^{2\alpha_{\mathrm{HN}}} + 2\left(\frac{\tau}{\tau_{\mathrm{HN}}}\right)^{\alpha_{\mathrm{HN}}} \cos(\pi\alpha_{\mathrm{HN}}) + 1\right)^{\frac{\beta_{\mathrm{HN}}}{2}}}, \quad (5)$$

where

$$\Theta = \arctan\left(\frac{\sin(\pi\alpha_{\mathrm{HN}})}{\left(\frac{\tau}{\tau_{\mathrm{HN}}}\right)^{\alpha_{\mathrm{HN}}} + \cos(\pi\alpha_{\mathrm{HN}})}\right)$$

and $0 \le \Theta \le \pi$.

Here, α_{HN} and β_{HN} represent the variables responsible for halfwidth and asymmetry of the feature written as the peak of $g_{\mathrm{HN}}(\tau)$, and τ_{HN} ensures the peak position on the frequency scale.

Disadvantage of this weight function option is in the fact that the GN function (5) contains only two variables: α_{HN} and β_{HN} and this, generally speaking, considerably restricts the capability of varying its form when analyzing the experimental data.

Figure 3 illustrates a series of $g_{\mathrm{HN}}(\tau)$ curves (in the linear and logarithmic scales) corresponding to some set of values of α_{HN} and β_{HN}. The curves show that downward deviation of α_{HN} from 1 activates slow relaxers in the design model, i.e. results in the growth of relative contribution of the slow relaxers with longer relaxation times (Figure 3, *a*). Instead, downward deviation of another variable,i.e. downward deviation of β_{HN} from 1, activates fast relaxers, i.e. results in the growth of relative contribution of fast relaxers with short relaxation times (Figure 3, *b*).

Thus, the primal problem of the DS form calculation is solved by substituting function (5) into expression (1) for various values of α_{HN} and β_{HN} lying within the range from 0 to 1 and ensuring the best agreement between the integration result and the experiment. The inverse problem — finding the best form of $g_{\mathrm{HN}}(\tau)$ — may be solved, for example, by repeatable solution of the primal problem with varying the specified variables and gradual updating their values in order to find the best agreement between the calculations and measurements.

Figure 4 shows the influence of the variation of α_{HN} and β_{HN} described above on the form of DS features. Comparison of DS calculated using equation (1) containing the relaxer distribution in the form of the GN function with the Debye distribution (2) shows that the design features of DS with comparably low time (and, accordingly, frequency) width ($\tau/\tau_{\mathrm{HN}} \approx 0.6$ at $\alpha_{\mathrm{HN}} = 0.9$, $\beta_{\mathrm{HN}} \approx 1$) are shifted in the peak into the low-frequency region by approx. 1 kHz from point $(\tau/\tau_{\mathrm{HN}}) = 1$ (Figure 4, *a*). In this case, 65% of the relaxer array appears to be shifted towards longer times, i.e. into the low-frequency region. At the same time, wider design features of DS on the time (and, accordingly, frequency) scale ($\tau/\tau_{\mathrm{HN}} \approx 2.5$, $\alpha_{\mathrm{HN}} < 0.7$, $0 < \beta_{\mathrm{HN}} < 1$) are even more shifted into the low-frequency region: to 1.7 kHz from point $(\tau/\tau_{\mathrm{HN}}) = 1$. In this case, as many as 85% of the relaxer time array appears to be shifted towards the longer times. This effect is associated with inadequately quick decline of the GN function towards longer relaxation times, i.e. this function is unproportionally high at times longer than τ_{HN}. Variations of α_{HN} downwards to $\alpha_{\mathrm{HN}} = 0.5$ and $\alpha_{\mathrm{HN}} = 0.3$ (that may be required at the fitting stage) result in an unacceptable result: the Debye frequency $f = 1/(2\pi\tau_{\mathrm{HN}})$ appears to be by an order of magnitude higher than $f_{\max}$ of the peak of the calculated DS features.

On the other hand, the calculations show that a decrease in the second variable β_{HN} at high constant value of α_{HN} results in drastically other calculation result. For example, at$\alpha_{\mathrm{HN}} = 0.98$ and $\beta_{\mathrm{HN}} = 0.5$ (and especially at $\beta_{\mathrm{HN}} = 0.3$), the DS features calculated using equation (1) during the integration broaden (Figure 4, *b*) and their peak is shifted into the high-frequency region (short time region), rather than into the low-frequency region, with respect to the Debye distribution; the same also takes place for 90% of the total relaxer array.

In view of the foregoing, an idea naturally arises to use the simultaneous variation of both α_{HN} and β_{HN} to get the

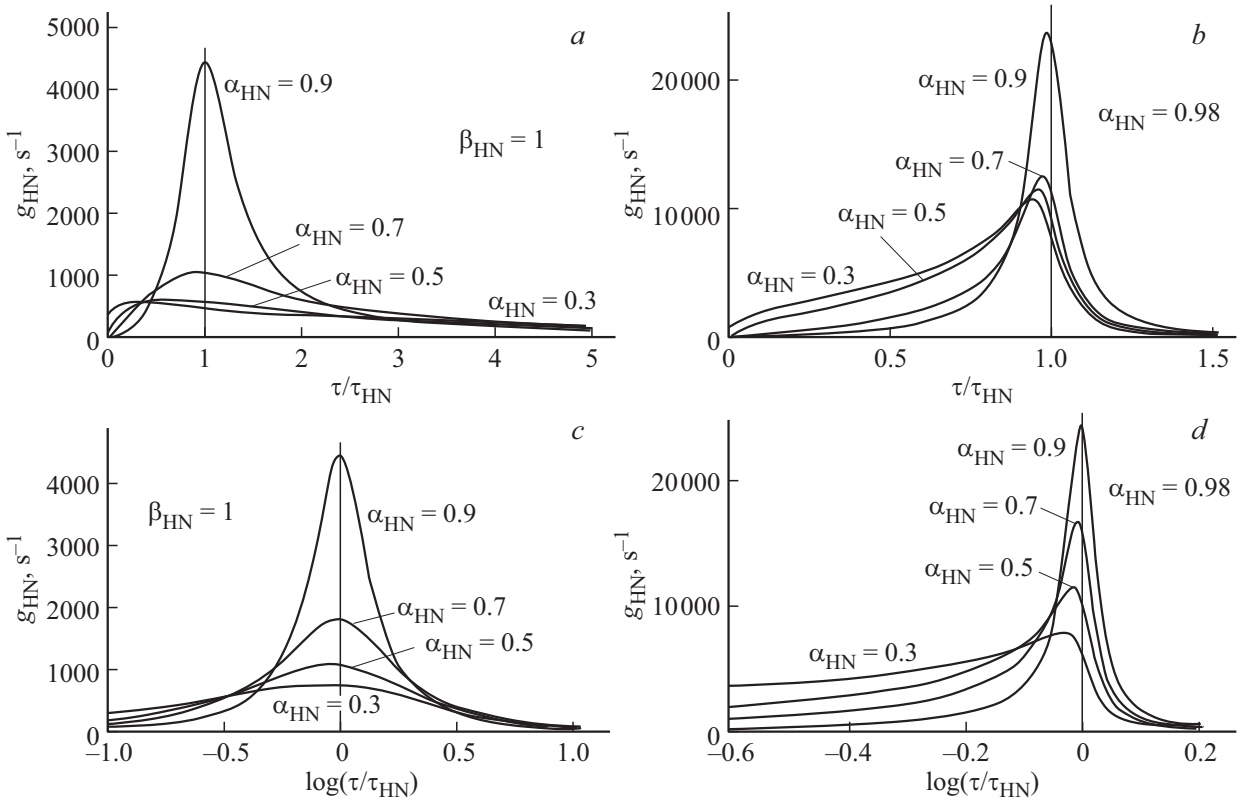

Figure 3. Gavrilyak–Negami functions in the linear scale $g_{HN}(\tau/\tau_{HN})$ (*a* and *b*) and logarithmic scale $g_{HN}(\log\tau/\tau_{HN})$ (*c* and *d*) at different values of α_{HN} and β_{HN}. $\tau_{HN} = 1.6 \cdot 10^{-4}$ s.

best results of fitting between the design and experimental curves. However, this method has critical disadvantage, i. e. agreement between the calculation and experimental data provided through simultaneous variation of α_{HN} and β_{HN} is achieved for wide (twice as wide as the Debye width) DS features at various combinations of numerical values of these variables, which induces fitting uncertainty. Specifically, an important question remains unanswered: whether a particular combination of α_{HN} and β_{HN} and the distribution $g_{HN}(\tau)$ given by it are physically justified or are inadequate to the experimental data due to the uncertainty mentioned above. The foregoing suggests that the above method for solution of the inverse problem of finding the relaxer distribution function $G(\tau)$ through repeated solution of the primal problem contains an ambiguity of result to be obtained.

6. Improved GN function

Considering the foregoing, it is reasonable to address a more advanced option to achieve the acceptable agreement between the calculation and experiment by using an improved GN function instead of $G(\tau)$. The improvement is reduced to multiplying function (5) by the Gaussian exponent with introduction of two additional adjustable variables η and γ: $G(\tau) = g_{HN}(\tau) \cdot \exp[(\tau - \eta)^2/\gamma^2]$. Such multiplication allows suppression of $G(\tau)$ values at high $\tau > \tau_{HN}$ to ensure almost symmetrical form of the function. For comparison, Figure 5 shows the results of calculations using equation (1) for $g_{HN}(\tau) - a)$ and $g_{HN}(\tau) \cdot \exp[(\tau - \eta)^2/\gamma^2] - b)$. It appears that the use of the symmetrical form of the distribution function $G(\tau)$ with halfwidth τ_{HN} ($\tau_{HN} = 2.3 \cdot 10^{-4}$ s, $\alpha_{HN} = 0.6$, $\beta_{HN} = 1$, $\eta = \tau_{HN}$, $\gamma = 0.7 \cdot \tau_{HN}$) avoids the low-frequency shift of the calculation data from point $\tau/\tau_{HN} = 1$ and brings the calculated DS features back into the high-frequency region and, thus, a much better agreement with the Debye frequency $f = 1/(2\pi\tau_{HN})$ is achieved for their frequency position (Figure 5, *b*). However, the calculated DS features themselves still have the same inadequately narrow frequency range as the Debye distribution itself. And only by means of a quite considerable expansion of the relaxer distribution region as specified for the integration ($\tau_{HN} = 2.3 \cdot 10^{-4}$ s, $\alpha_{HN} = 0.6$, $\alpha_{HN} = 0.1$, $\eta = 2 \cdot \tau_{HN}$, $\gamma = 3 \cdot \tau_{HN}$), a width of the DS features close to the experimental width may be achieved through calculation. It should be noted again that the result which is adequate to the experiment — wide DS features and rational peak position — has been achieved by this option using the improved function $G(\tau) = g_{HN}(\tau) \cdot \exp[(\tau - \eta)^2/\gamma^2]$ that differs qualitatively from the previous option $G(\tau) = g_{HN}(\tau)$. This additionally confirms the conclusion that the solution of the inverse problem of finding $G(\tau)$ is ambiguous.

Figure 5 shows $G(\tau)$ vs. τ/τ_{HN} and vs. $\log(\tau)$. Emphasis shall be made on an important consideration that this

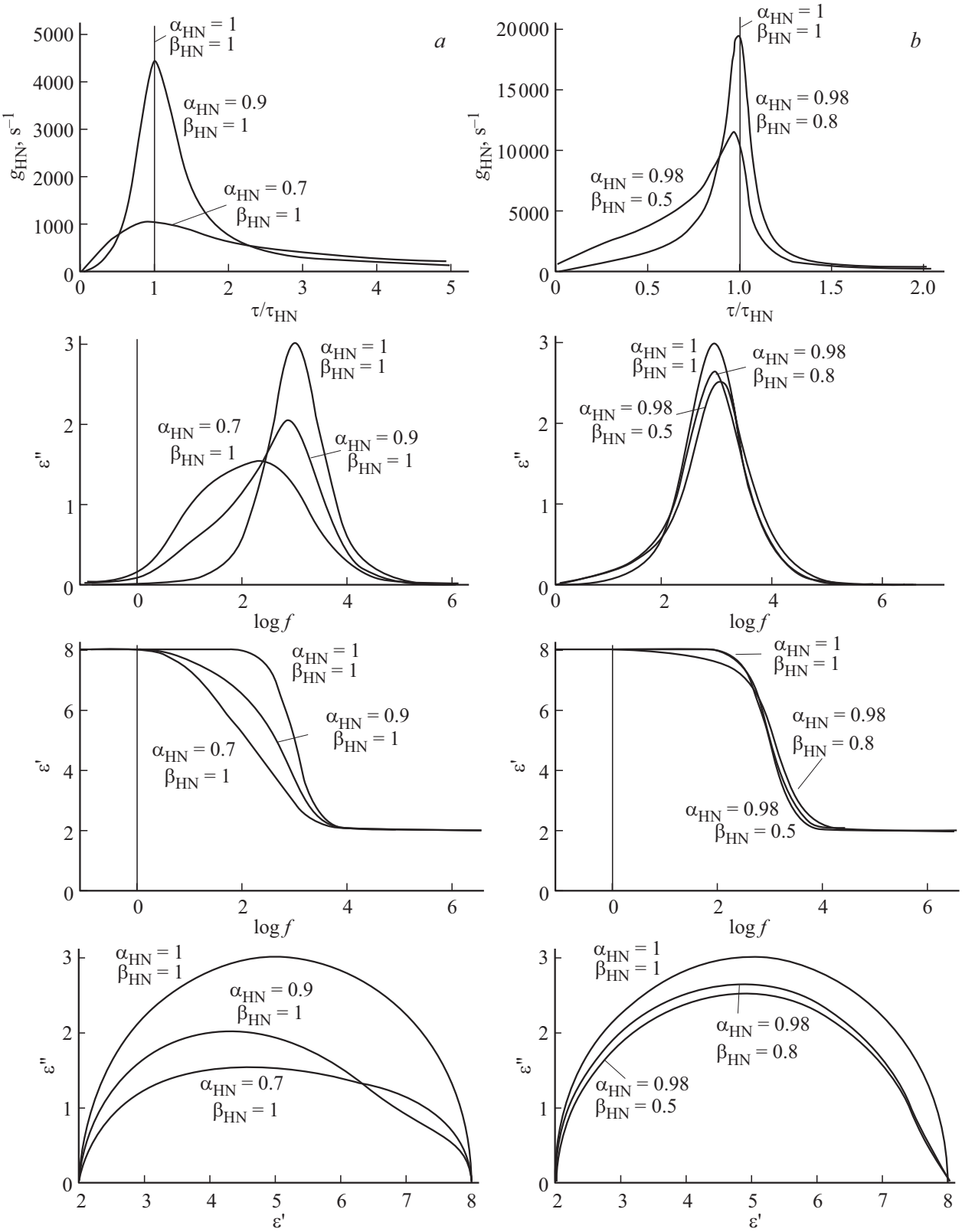

Figure 4. *a*) The GN function ($\tau_{HN} = 1.6 \cdot 10^{-4}$ s, $\alpha_{HN} = 0.9$, $\beta_{HN} = 1$ and $\alpha_{HN} = 0.7$, $\beta_{HN} = 1$) and the frequency dependences $\varepsilon'(f)$, $\varepsilon''(f)$ and CC diagrams $\varepsilon''(\varepsilon')$ with a single feature of DS plotted using the GN function by equation (1). The frequency curves are given in comparison with the design curves according to equation (2): $\alpha_{HN} = 1$, $\beta_{HN} = 1$. *b*) The GN function ($\tau_{HN} = 1.6 \cdot 10^{-4}$ s, $\alpha_{HN} = 0.98$, $\beta_{HN} = 0.8$ and $\alpha_{HN} = 0.98$, $\beta_{HN} = 0.5$) and the frequency dependences $\varepsilon'(f)$, $\varepsilon''(f)$ and CC diagrams $\varepsilon''(\varepsilon')$ with a single feature of DS plotted using the GN function by equation (1). The frequency curves are given in comparison with the design curves according to equation (2): $\alpha_{HN} = 1$, $\beta_{HN} = 1$.

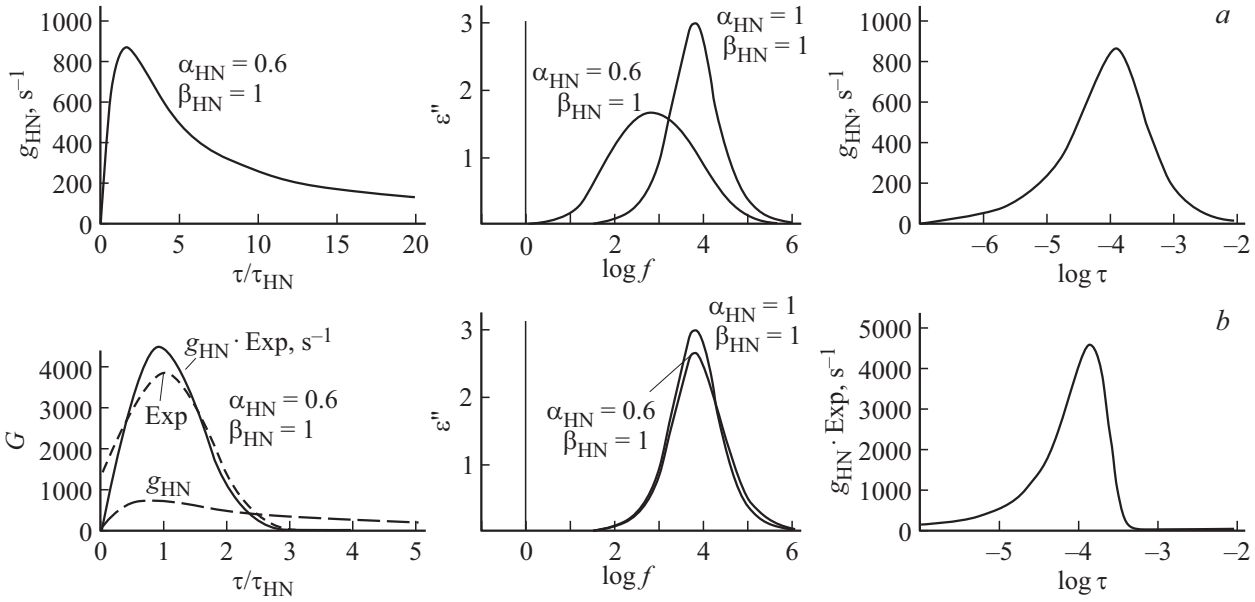

Figure 5. Results of calculations using equation (1) for the imaginary part of permittivity $\varepsilon(f)$ considering the distribution function g_{HN} ($\tau_{HN} = 2.3 \cdot 10^{-4}$ s, $\alpha_{HN} = 0.6$, $\beta_{HN} = 1$) — *a*, and improved function $G(\tau) = g_{HN} \cdot \exp[(\tau - \eta)/\gamma]^2$ ($\eta = 2 \cdot \tau_{HN}$, $\gamma = 3 \cdot_{HN}$) — *b*. Curves for the design dependences $\varepsilon''(f)$ are given in comparison with the design curves according to equation (2): $\alpha_{HN} = 1$, $\beta_{HN} = 1$. Distribution functions are shown in the linear and logarithmic scales.

function is used not only for integration by equation (1), but also almost coincides in form in the logarithmic scale with the calculated frequency dependence of the imaginary part of permittivity$\varepsilon''(f)$ and with the mirror reflection of the curve relative to the horizontal axis!

This similarity has a rational explanation. In particular, the Debye function $\varepsilon''(f)$ outline, that is relatively narrow in frequency and plays a role of the filtering function (similar to the filtering property of the Diracδ-function) under the integral (1), after integration using equation (1), draws the outline of $G(\tau)$ curve, but only in the direction mirrored with respect to the initial direction. Mirroring occurs because $\omega = 1/\tau$ and $\log(\tau) = -\log(\omega)$.

7. Using modified measurements of $\varepsilon''(f)$ as $G(\tau)$

The final construction stage of the specified mathematical model uses an experimental data array for the values of the imaginary part of the frequency dependence function of permittivity $\varepsilon''(f)$ as an option of finding $G(\tau)$. Such method is based on the fact that the experimental function $\varepsilon''(f)$ contains concealed information on the rate of response of the oscillation system to an external sinusoidal impact, i. e. on the density of system relaxation time distribution on the frequency (and, accordingly, time) scale. Hence, after replacement of f with τ ($f = 1/2\pi\tau$), $\varepsilon''(\tau)$ may be used (after normalization) as an inoculating function for utilization in expression (1) as $G(\tau)$ — relaxer-time distribution function.

The Debye function, having a low halfwidth, may be successfully used as a filtering function, but only for quite wide DS features compared with it. Nevertheless, comparison of such calculation data with the experimental data shows that the calculated peak has a lower height and a higher frequency width than those of the experimental peak. Therefore, correction of the relaxer-time distribution function is required: for example, the number of low-frequency relaxers shall be decreased and the number of medium- and high-frequency relaxers shall be increased. Thus, the use of the Debye function that is asymmetrical (as opposed to the commonly used filters in the form of symmetrical approximations to the Dirac δ-function) requires the parameters of $\varepsilon''(\tau) = G(\tau)$ to be updated when fitting to the experimental data to achieve the best coincidence of the calculation using equation (1) with the experimental data. The modern dielectric spectrometer software solves this problem by numerical methods. The required $G(\tau)$ provided by the spectrometer looks like a data array that may be used to plot the curves of this function both in linear and logarithmic scales. It should be noted again that for the DS features with wide frequency range, the experimental function $\varepsilon''(f)$ and calculated function $G(\tau)$ represented in the logarithmic scales almost coincide in a mirror-like manner with each other.

8. Conclusion

Thus, the calculations performed herein suggest that the inverse problem of finding the form of relaxer-time distribution function $G(\tau)$ has no unambiguous solution.

The GN function may be used as a good approximation at the preliminary stage of finding the form of $G(\tau)$ in expression (1) for narrow experimental DS features

compared with the Debye distribution. For wider DS features, an improved function (for example, $g_{\mathrm{HN}} \cdot \exp$) must be used. And finally, for the widest DS features, a rational result as $G(\tau)$ is provided by the experimental function $\varepsilon''(f)$ with replacement of f with τ. After this, $\varepsilon''(\tau)$ may be used as an inoculating function (6) for expression (1) with subsequent correction of the form of the function.

Besides the foregoing, another cause of broadening of the DS features shall be considered, i. e. attenuation of the relaxation oscillation amplitude in a specific physical medium due to the loss of oscillation energy.

A set of physical reasons behind a specific form of the experimental DS features can be certainly identified only through in-depth interpretation of measurements with involvement of all available additional data on the test material: type, properties and concentration of various impurities, degree of defects in the studied material, etc.

Conflict of interest

The authors declare that they have no conflict of interest.

References

[1] A.M. Prokhorov. Dielekticheskie izmereniya. Sov. entsiklopediya, M. (1988). T. 1. P. 700. (in Russian).
[2] A.A. Volkov, A.S. Prokhorov. FTP **46**, *8*, 657 (2003). (in Russian).
[3] R. Richert. Adv. Chem. Phys. **156**, 101 (2015).
[4] A.S. Volkov, G.D. Koposov, R.O. Perfil'ev, A.V. Tyagunin. Optika i spektroskopiya **124**, *2*, 206 (2018). (in Russian).
[5] A.S. Volkov, G.D. Koposov, R.O. Perfilyev. Optika i spektroskopiya **125**, *3*, 364 (2018). (in Russian).
[6] A.I. Gusev. Osnovy dielekticheskoy spektoskopii. Kazan (2008). P. 112. (In Russian).
[7] D.N. Chausov. Liq. Cryst. Appl. **18**, *3*, 45 (2018).
[8] A.M. Maharramov, R.S. Ismailova, M.A. Nuriyev, A.A. Nabiyev. Plastics **1**, 1 (2019).
[9] D.S. Anikonov, D.S. Konovalova. Sib. mat. zhurn. **43**, *987*, 387 (2002). (in Russian)
[10] K.S. Cole, R.H. Cole. J. Chem. Phys. **99**, *4*, 341 (1941).
[11] S. Havriliak, S. Negami. J. Polym. Sci. **14**, 99 (1966).
[12] Yu.I. Yurasov, A.V. Nazarenko. Nauka Yuga Rossii **14**, *4*, 35 (2018). (in Russian)
[13] R.O. Perfilyev, G.D. Koposov, A.S. Volkov. Vestn. Severnogo Federal'nogo un-ta im. M.V. Lomonosova (2017). (in Russiaon). P. 155–156.
[14] K.G. Bogolitsyn, S.S. Khviyuzov, A.S. Volkov, G.D. Koposov, M.A. Gusakova. Zhurn. fiz. khimii **93**, *2*, (2019). (in Russian).
[15] P.A.M. Dirac. Lectures on Quantum Field Theoty, N.Y. (1967) P. 234.
[16] P.A.M. Dirac. Printsipy kvantovoy mekhaniki. Mir, M. (1968) P. 481. (in Russian)
[17] A.N. Kolmogorov, S.V. Fomin. Elementy teorii funktsiy i funktsional'nogo analiza. Nauka, M. (1968), P. 496. (in Russian).
[18] I.M. Gelfand, G.E. Shilov. Oboshchennye funktsii i deistviya nad nimi. Gos. izd-vo fiz.-mat. li-ry (1959) P. 472. (in Russian).

Translated by E.Ilinskaya